Biodistribution of Indium-111-Labeled Antibody Directed Against Intercellular Adhesion Molecule-1

Daniel E. Sasso, Maria A. Gionfriddo, Roger S. Thrall, Sergei I. Syrbu, Henry M. Smilowitz and Ronald E. Weiner
Departments of Nuclear Medicine, Medicine, Surgery and Pharmacology, University of Connecticut Health Center, Farmington, Connecticut

We examined the biodistribution in normal rats of an ^{111}In-labeled mouse monoclonal antibody to rat intercellular adhesion molecule-1 (^{111}In-aICAM-1), as a potential detector of inflammation. **Methods:** Indium-111-aICAM-1 or ^{111}In-labeled normal mouse polyclonal immunoglobulin G (^{111}In-nmIgG) was injected into rats. Groups of three to four rats were killed up to 18 hr after injection, and activity was measured in various tissues. Rats were also imaged at 1 and 18 hr after injection. **Results:** Uptake of ^{111}In-aICAM-1 was greatest in the lung (~10% injected dose [ID]/g at 15 min) and then declined steadily (to ~2% ID/g at 18 hr). Lung uptake of ^{111}In-nmIgG was eightfold less than that for ^{111}In-aICAM-1 and did not change throughout the 18 hr. At all time points, blood activity for ^{111}In-aICAM-1 was only 30% to 40% of that for ^{111}In-nmIgG, whereas the percent injected dose per gram was increased more than twofold in the major organs. Compared with ^{111}In-nmIgG, the ^{111}In of aICAM-1 was shifted from the blood and was distributed among the lung, kidney, spleen and liver. **Conclusion:** Indium-111-aICAM-1 may be useful as an early inflammation detection agent. Intercellular adhesion molecule-1 upregulation is a very early event in inflammation and rapid removal from the blood of this antibody provides low background in contrast to the usual high background with whole antibodies.

Key Words: intercellular adhesion molecule-1; indium-111; anti-intercellular adhesion molecule-1 antibody

J Nucl Med 1996; 37:656–661

Within hours of the beginning of an inflammatory process, the site is invaded with large numbers of polymorphonuclear leukocytes (PMNs) (*1*). The PMNs first bind to endothelial cells in the neighborhood of the inflammation and then move to a junction between cells and squeeze through into the interstitial space. In the past few years, the molecular details of this process have begun to emerge (*2–5*). An essential component of this process is the expression of three families of adhesion molecules—the integrin, immunoglobulin supergene and selectin families—on both the PMNs and endothelial cells (*3,5,6*). One integrin, leukocyte function-associated antigen-1 (LFA-1), present on the neutrophil surface, binds to intercellular adhesion molecule-1 (ICAM-1), expressed on the surface of the endothelial cell. Both are expressed at low basal levels but are upregulated by a variety of proinflammatory agents, such as chemotactic peptides, endotoxin and cytokines. This upregulation is associated with increased PMN adhesiveness to endothelial cells and transendothelial migration (*4,7,8*).

The availability of molecular probes such as monoclonal antibodies to various adhesion molecules could be useful in nuclear medicine. These adhesion molecules are increased early, before the influx of PMNs, in a variety of inflammatory processes. Thus, anti-adhesion molecule antibodies have the potential to provide new, more specific diagnostic agents that could be earlier predictors of inflammation than ^{111}In-PMN or ^{67}Ga-citrate, the agents commonly used at present. Recently, in preliminary animal experiments, a monoclonal antibody directed against E-selectin, an adhesion molecule present on endothelial cells only during inflammation, showed promise in detecting joint inflammation (*9*). Also, understanding the molecular details of leukocyte–endothelial cell interaction should aid in understanding the distribution and recruitment of the widely used ^{111}In-PMN.

In an initial study to determine whether an ^{111}In-labeled mouse anti-rat ICAM-1 (aICAM-1) might be a suitable inflammation detection agent, we examined the biodistribution of ICAM-1 in normal rats. In the lung there is initially a high concentration of ^{111}In that is substantially reduced as a function of time. The activity is very rapidly removed from the blood and concentrated in the major organs, yielding low background.

MATERIALS AND METHODS

Preparation of Indium-111-Labeled Antibody

The coupling of cyclic anhydride DTPA to either mouse immunoglobulin (Ig) G_1 monoclonal aICAM-1 or normal mouse polyclonal IgG (nmIgG) was performed according to Paik et al. (*10*). Cyclic anhydride DTPA in anhydrous dimethyl sulfoxide was added to the antibody solution (5–15 mg/ml) in a 5–30:1 ratio to yield 0.7–1.2 DTPA for each protein. To remove unbound DTPA, 100–200 μl of the IgG–DTPA solution was washed three times with 2 ml of 50 m*M* PIPES containing 100 m*M* NaCl, pH 6.5 (PIPES buffer), using a Centricon-30 microconcentrator. To add ^{111}In to the IgG–DTPA solution, an ^{111}In-nitrilotriacetic acid (NTA) solution was made by titrating acidic ^{111}InCl-NTA solution to pH 6.5 and incubating for 30 min at 80°C. Then, 5–50 μl of this mixture (approximately 1 m*M* NTA) was added to the IgG–DTPA solution in PIPES buffer, pH 6.5, and incubated for 1 hr or overnight at 37°C. Nonbound ^{111}In was removed with three washes with 0.9% NaCl using the Centricon-30. Before injection into the rats, this solution was passed through a 0.22-μm filter.

Assay for Binding of Labeled Antibodies to Endothelial Cells

Rat lung microvascular endothelial cells were grown in 96-well plates to confluence (6.8 ± 0.3 μg of cell membrane protein per well), and ICAM-1 expression was increased by stimulation with 10 μg/ml of lipopolysaccharide (LPS) (Sigma; Serotype O 128: B12) for 24 hr. The cells were fixed for 15 min at room temperature with 1% paraformaldehyde, washed twice with phosphate-buffered saline (PBS), pH 7.4, and incubated for 40 min with blocking solution (2.5% bovine serum albumin [BSA] in PBS). All wells then received aliquots of blocking solution containing either ^{111}In-aICAM-1 or ^{111}In-nmIgG (10 ng per well) and were incubated for various times (Fig. 1A). Each assay was performed in quadruplicate. Nonspecific binding was assessed by pretreating control wells with 200 ng per well of unlabeled aICAM-1 or nmIgG. To determine the amount of antibody bound, the wells were washed four times with PBS; the cell monolayer was

Received Feb. 7, 1995; revision accepted Jun. 7, 1995.
For correspondence or reprints contact: Ronald Weiner, PhD, University of Connecticut Health Center, Nuclear Medicine MC-2804, 263 Farmington Ave., Farmington, CT 06030.

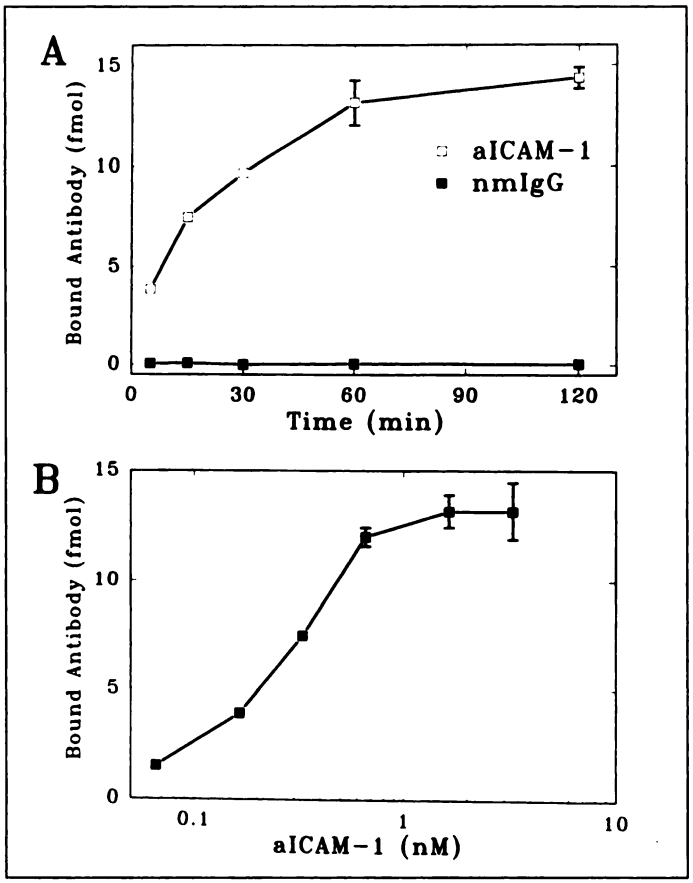

FIGURE 1. (A) Ability of ^{111}In-aICAM-1 and ^{111}In-nmIgG to bind to rat lung microvascular cell membrane protein. Bound activity determined at different times is shown. (B) Influence of ^{111}In-aICAM-1 concentration on binding to membrane protein. Bound activity was determined after 2 hr of incubation. Data shown are mean ± s.d. of quadruplicate samples.

solubilized with 150 μl of 10% sodium dodecyl sulfate; and the amount of radioactivity was measured. To determine the affinity constant of ^{111}In-aICAM-1 for the cells, the antibody concentration was varied (Fig. 1B), the samples were incubated for 2 hr, and the plates were processed as described before.

Biodistribution of ^{111}In-Labeled Antibodies in Rats

Pathogen-free Fischer 344 male rats from Charles River Laboratories (Worthington, MA), weighing 200–225 g, were anesthetized, and each animal received an intravenous (i.v.) injection of 0.122–0.229 MBq (3.3–6.2 μCi) containing 10 μg of mouse monoclonal ^{111}In-aICAM-1 or, as a control, ^{111}In-nmIgG. The animals were killed at 15 and 30 min and 1, 4 and 18 hr (three to four rats per group) after injection. Whole organs (lung, kidney, liver, spleen and heart) and a portion of the intestines were removed and weighed, and activity was measured. Total blood was estimated at 6.41% of body weight (*11*). Data are expressed as both percent injected dose (ID) per gram of tissue and percent ID per organ.

The labeling of the same lot of nmIgG with DTPA at different times had no significant effect on the biodistribution of ^{111}In except for the amount deposited in the kidney, which resulted in a higher percent coefficient of variation (CV) (20%–25%) than that for the other tissues, (7%–20%). Different lots of aICAM-1 appeared to cause a variation in the percent ID per gram for lung and major organs. On further analysis, this variation was actually caused by a redistribution of ^{111}In-aICAM-1 between the blood and these tissues. This redistribution may reflect variable expression of ICAM-1 in the lung and other tissues of rats from different shipments. Because of these considerations, we chose to display curves that demonstrate the minimum differences between the biodistributions of ^{111}In-aICAM-1 and ^{111}In-nmIgG.

Immunofluorescence

Lungs were processed as previously described (*12*). Briefly, lungs were excised, prepared for routine cryostat sectioning and cut into 5-μm frozen sections. The sections were fixed in acetone (−20°C) for 2 min, dried and placed in blocking solution (PBS containing 5% milk and 5% BSA) for 30 min at room temperature. First, antibody was added in blocking solution for 1 hr followed by three 5-min washes in PBS. Rhodamine-conjugated goat anti-mouse IgG was incubated for 1 hr followed by three 5-min washes in PBS. Fluorescent images were acquired from a Zeiss LSM 410 confocal laser scanning microscope using a 40× neofluor lens (numerical aperture 1.3).

Imaging of ^{111}In-Labeled Antibodies in Rats

Anesthetized rats received an i.v. injection of 2.2 MBq (60 μCi) containing 10 μg of either ^{111}In-aICAM-1 or ^{111}In-nmIgG. At 1 and 18 hr after injection, the rats were imaged using a Siemens Orbiter gamma camera with a Micro Delta computer. A pinhole collimator was used for each anterior image of the upper torso, which took approximately 10 min per image (100,000 counts). Anterior images of the whole animal were obtained with a LEAP collimator, and 50,000 counts were collected.

Statistical Analysis

The Student's unpaired t-test was used to test the differences between mean values. Linear regression analysis was used to analyze the data for the Scatchard method.

RESULTS

Specificity of Indium-111-ICAM-1

To determine whether labeling the antibody with ^{111}In interfered with the ability of the aICAM-1 to interact with the antigen, the labeled antibody was incubated with rat microvascular cells previously treated with LPS to upregulate ICAM-1. Figure 1A shows binding of ^{111}In-aICAM-1 to these cells and that the amount of Ig bound leveled off after 120 min of incubation. In control experiments, no binding of ^{111}In-nmIgG was found. To determine whether ^{111}In-aICAM-1 antibody binding achieves saturation, the antibody concentration was varied, whereas the number of cells remained fixed. Antibody saturation was observed, and no detectable binding of ^{111}In-nmIgG was found under these conditions (Fig. 1B). These data were analyzed using the Scatchard method, and an affinity constant K_a of 0.46 ± 0.19 × 10^9 was determined for the ^{111}In-aICAM-1.

Biodistribution of Indium-111-aICAM-1 and ^{111}In-nmIgG

At 15 min after injection, lung uptake of ^{111}In-aICAM-1 was greatest for all tissues, almost 10% ID/g (Fig. 2A), and then declined dramatically to little more than 2% ID/g at 18 hr. The decrease, however, in the lung/blood ratio was more moderate, with a decline from 4.4 to 3.6 at the later time point. Injection of ^{111}In-nmIgG gave a starkly different result. Lung uptake did not change up to 18 hr ($p > 0.1$).

There were also dramatic differences between the two immunoglobulins in percent ID per gram of the major organs. Compared with ^{111}In-nmIgG, the activity of ^{111}In-aICAM-1 was shifted from the blood and was distributed among the lung, kidney, spleen and liver (Fig. 2). At all time points, blood activity for ^{111}In-aICAM-1 was only 30%–40% of that for ^{111}In-nmIgG ($p < 0.05$) (Fig. 2A). At the earliest time point (15 min), the most substantial increase (more than ninefold, $p < 0.001$) in ^{111}In-aICAM-1 was in lung tissue compared with that for ^{111}In-nmIgG. At all later time points, ^{111}In-aICAM-1

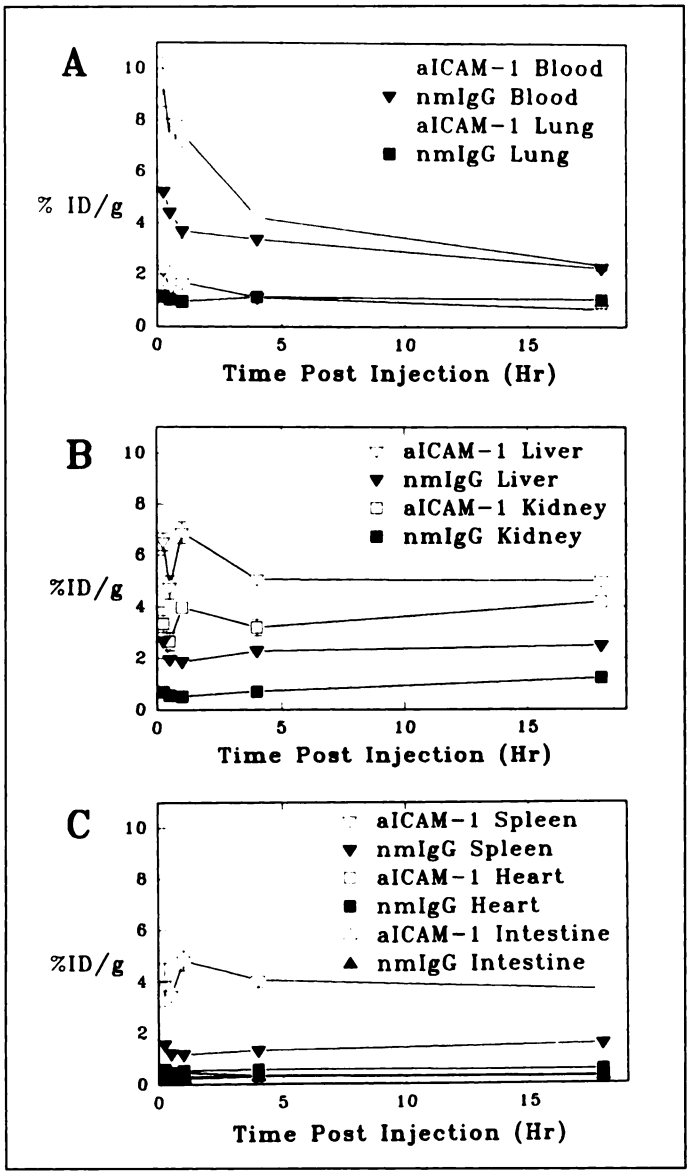

FIGURE 2. Tissue clearance of ^{111}In-nmIgG and ^{111}In-aICAM-1 in rats. Data shown are mean ± s.d. of tissues from three to four rats.

activity in the lung was also greater than ^{111}In-nmIgG activity ($p < 0.05$). When the other tissues were compared, liver activity of ^{111}In-aICAM-1 was increased more than twofold ($p < 0.001$), kidney activity threefold to fourfold ($p < 0.001$) and spleen activity twofold to fourfold ($p < 0.002$) that of ^{111}In-nmIgG for all time points (Fig. 2, B and C).

Whole-organ incorporation data also confirmed that activity in rats injected with ^{111}In-aICAM-1 was rapidly removed from the blood and was deposited in organs other than the liver. In contrast, for rats injected with ^{111}In-nmIgG, ^{111}In left the blood more slowly, typical of whole antibody, and the liver was the major depository for activity. For example, at 1 hr after injection of ^{111}In-aICAM-1, less than 25% of the ID was still in the blood (Table 1) compared with more than 50% of that for ^{111}In-nmIgG ($p < 0.001$) (Table 2). More than 50% of the ID was present in the liver of rats injected with ^{111}In-aICAM-1, but only 16% was present in those injected with ^{111}In-nmIgG ($p < 0.001$). At 1 hr, the spleen, lung and kidney constituted 15% of the ID for ^{111}In-aICAM-1, but only 2.5% for ^{111}In-nmIgG ($p < 0.001$). At 4 hr, the total for these tissues declined to 11% for labeled aICAM-1 ($p < 0.001$) and increased slightly to 3% for labeled nmIgG ($p < 0.05$). The 18-hr value for ^{111}In-aICAM-1 did not change ($p > 0.5$, 18 hr versus 4 hr), but for ^{111}In-nmIgG there was a small but significant increase to 3.9 %ID/g ($p < 0.01$).

For the other tissues, there were small differences between the localization of the two antibodies as a function of time. In the liver, after the decline from the initial value to the 4-hr value ($p < 0.0002$), the percent ID per gram for ^{111}In-aICAM-1 was stable up to 18 hr (Fig. 2B). Localization of ^{111}In-nmIgG in the liver was slightly different. At 4 hr, there was a modest increase, which continued up to 18 hr. Labeled aICAM-1 uptake by the kidney showed a trend of increasing localization (4 hr versus 18 hr, $p < 0.001$) that may reflect deposition of catabolic products. For labeled nmIgG, the increase in ^{111}In activity in the kidney was significant ($p < 0.001$) but more moderate (1.3-fold

TABLE 2
Time Course of Organ Biodistribution (%ID per Organ) of Indium-111-labeled nmIgG in Normal Rats

	Time postinjection (mean ± s.d., n = 4)				
Tissue	15 min	30 min	1 hr	4 hr	18 hr
Lung	1.0 ± 0.07	1.0 ± 0.08	0.9 ± 0.08	1.0 ± 0.09	0.9 ± 0.36
Blood	71.6 ± 2.3	64.9 ± 3.1	54.1 ± 3.2	49.4 ± 4.4	32.6 ± 1.4
Kidney	1.1 ± 0.2	0.9 ± 0.20	0.9 ± 0.3	1.2 ± 0.06	2.1 ± 0.1
Spleen	0.9 ± 0.1	0.8 ± 0.07	0.7 ± 0.07	0.8 ± 0.1	0.9 ± 0.06
Heart	0.4 ± 0.03	0.3 ± 0.01	0.4 ± 0.04	0.4 ± 0.06	0.4 ± 0.07
Liver	21.1 ± 1.8	16.8 ± 1.3	16.1 ± 1.7	20.0 ± 1.4	22.1 ± 0.6
Total	96 ± 4	85 ± 5	73 ± 5	73 ± 6	59 ± 3

TABLE 1
Time Course of Organ Biodistribution (%ID/Organ) of Indium-111-Labeled Anti-ICAM in Normal Rats

	Time postinjection (mean ± s.d., n = 4)				
Tissue	15 min	30 min	1 hr	4 hr	18 hr
Lung	8.3 ± 0.7	6.4 ± 1.0	6.7 ± 0.2	3.5 ± 0.07*	2.0 ± 0.2
Blood	28.3 ± 4.1†	18.4 ± 1.6†	21.6 ± 1.2†	14.4 ± 1.5†	8.5 ± 0.9†
Kidney	5.0 ± 0.2	3.8 ± 0.4	5.8 ± 0.2	5.0 ± 0.2	6.7 ± 0.2
Spleen	2.1 ± 0.4	1.9 ± 0.16	2.5 ± 0.2	2.2 ± 0.1	2.2 ± 0.2
Heart	0.3 ± 0.02	0.2 ± 0.03	0.3 ± 0.02	0.2 ± 0.0	0.2 ± 0.02
Liver	51.5 ± 4.0†	36.3 ± 1.5†	54.5 ± 2.9†	42.7 ± 1.6†	39.9 ± 2.4†
Total	96 ± 7	67 ± 5	91 ± 4	68 ± 3	60 ± 2

*n = 3.
†$p < 0.001$ vs. analogous values in Table 2.

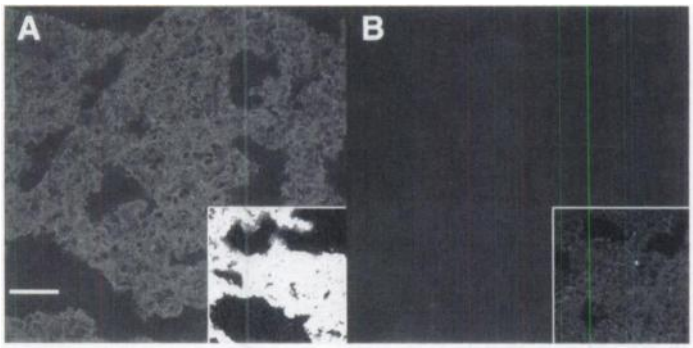

FIGURE 3. Immunofluorescence in cryostat sections of rat lung where (A) aICAM-1 was added first. (B) nmIgG was added first, and rhodamine-conjugated goat anti-mouse IgG was added second. Insets show a fourfold sample intensity increase. Magnification 788×.

increase) than that for labeled aICAM-1 (1.9-fold increase) from 4 to 18 hr. For all other tissues, there was no significant change in distribution during this time frame (Fig. 2C).

Immunofluorescence of aICAM-1 and nmIgG in Normal Rat Lung

Figure 3A shows that in lung tissue incubated with aICAM-1, the fluorescence is uniformly distributed, with small areas of higher intensity scattered throughout the tissue. In contrast, tissue incubated with nmIgG yielded almost no fluorescence (Fig. 3B). When the intensity of fluorescence was increased fourfold, the tissue structure in the control sample was more easily visualized (Fig. 3B, inset). These data imply that normal rat lung does indeed possess a high expression of ICAM-1 and correlate well with the high concentration of ^{111}In-aICAM-1 detected in lung.

Imaging of Indium-111-Labeled Antibodies in Rats

The whole-body images, at 1 hr (Fig. 4A) and 18 hr (Fig. 4B), of rats injected with ^{111}In-nmIgG and ^{111}In-aICAM-1 confirm the observations from tissue sampling. The scintigrams show an intense focus of ^{111}In activity in the spleen and liver. There is no observable localization in bone for either antibody. The greatest contrast between these images is the relatively high body background in the animals injected with ^{111}In-nmIgG compared with the low tissue and blood activity in the rats injected with ^{111}In-aICAM-1. The distinct character of these two antibodies expected from the biodistributions is also demonstrated in the pinhole images (Fig. 5). At 1 hr, the lungs of animals injected with ^{111}In-aICAM-1 are visible, and lung

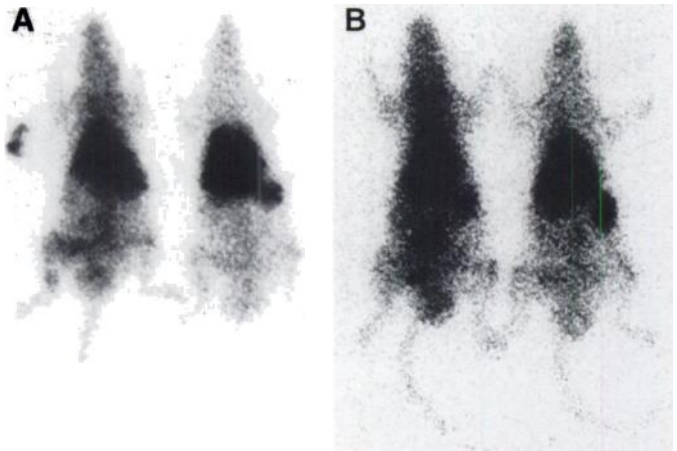

FIGURE 4. Whole-body scintigrams of rats injected with mouse ^{111}In-aICAM-1 (right) and ^{111}In-nmIgG (left) and imaged at 1 hr (A) and 18 hr (B) after injection.

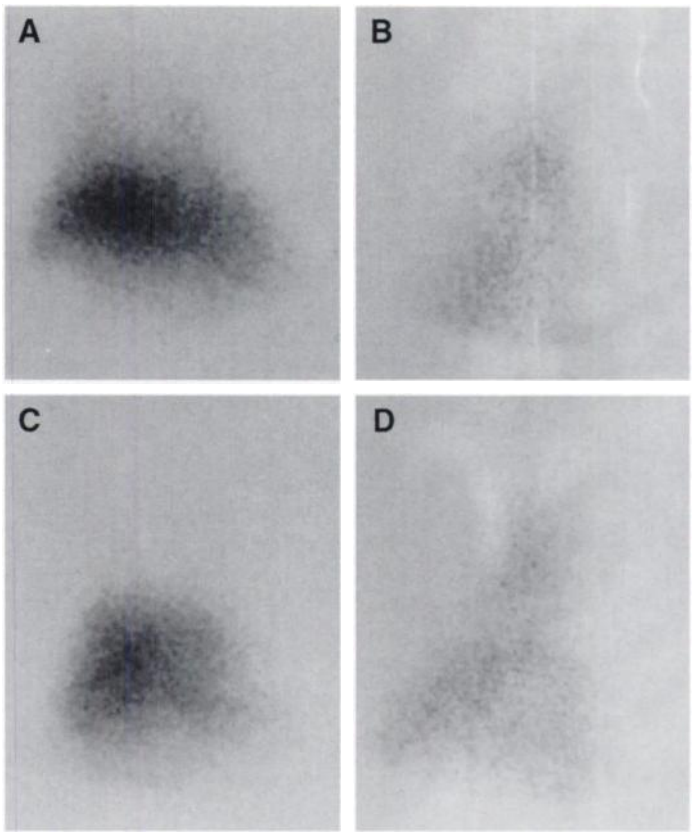

FIGURE 5. Pinhole scintigrams of rats injected with ^{111}In-aICAM-1 (A, C) and ^{111}In-nmIgG (B, D) and imaged at 1 hr (A, B) and 18 hr (C, D) after injection.

activity is greater than tissue background but lower than the intense liver activity (Fig. 5A). The 18-hr scintigram shows that the ^{111}In in the lung is reduced to near-background levels (Fig. 5C). The early image from the thoracic area of rats injected with ^{111}In-nmIgG shows only the cardiac blood pool, tissue activity and modest liver uptake (Fig. 5B), which did not appreciably change on the overnight images (Fig. 5D).

DISCUSSION

The present data suggest that ^{111}In-aICAM-1 does indeed map ICAM-1 expression in vivo. The covalent addition of a DTPA moiety does not appear to alter significantly the aICAM-1 structure. The K_a value for ^{111}In-aICAM-1 is within the usual range for antibody–antigen interactions considered high affinity (*13,14*). The disparate biodistribution between the two immunoglobulins implies a unique character for ^{111}In-aICAM-1. Indium-111-nmIgG has a biodistribution comparable to that of another undirected polyclonal IgG, human ^{111}In-IgG, in normal rats (*15,16*). In contrast, ^{111}In-aICAM-1 rapidly disappears from the blood and concentrates in the major organs. This concentration would be expected if the antigen was widely distributed in the liver, spleen, kidney and lung. The antibody would immediately saturate the available antigenic sites. In the absence of any stimuli, there is a low level of ICAM-1 expression on endothelial cells in culture (*17*). Moreover, ICAM-1 has been identified by immunohistological examination in normal human endothelial and fibroblast-like cells of the liver, kidney and intestines (*18*). High ICAM-1 presence has been detected in normal human lung vascular endothelium, with modest expression in the lung epithelial tissue (*19*). We observed a particularly high initial localization of ^{111}In-aICAM-1 in lung tissue that correlated well with the immunofluorescence studies with the unlabeled antibody. The immediate deposition of ^{111}In-IgA and ^{111}In-labeled anti-E-selectin in

major organs has been observed in other animal models and is thought to be a receptor-based process (*15,20*).

Indium-111-labeled anti-adhesion antibodies might be useful as a specific and early detector of inflammation. There are a variety of adhesion molecules involved in the recruitment of PMNs to sites of inflammation. One of the first steps in this process is the rolling of the PMN along the endothelial cells, which is mediated by upregulation of the selectin family (*2,6*). Critical for the next stage is the upregulation of ICAM-1 and upregulation and activation of its counterreceptor on the PMN $LFA\text{-}1_{alpha}$. This process allows the PMN to become firmly attached to the endothelial cell and then to migrate between the endothelial junction into the interstitium. White blood cells (WBCs) labeled with ^{111}In and ^{99m}Tc are commonly used for detection of inflammation. Some infections can be detected with ^{99m}Tc-labeled WBCs as early as 1–3 hr after injection (*21–23*). Because adhesion molecules are upregulated before the PMN influx, these molecules could be useful in a similar time frame. Keelan et al. (*9*) have shown the utility of using ^{111}In-labeled anti-E-selectin to detect inflammation in an animal model of arthritis. They demonstrated a fivefold increase in the localization ratio (inflamed versus noninflamed contralateral joint) when the anti-E-selectin antibody was compared with the control antibody, but imaging at 24 hr after injection was required.

Intercellular adhesion molecule-1 may be a better target ligand than E-selectin for early detection of inflammation because E-selectin upregulation is typically transient (initiates within 1–2 hr, reaches a maximum at 3–6 hr and returns to baseline by 24–72 hr) (*2,20,24,25*), whereas ICAM-1 upregulation is usually more long lasting (maximal at 8–10 hr; then ICAM-1 density remains elevated for 2–7 days) (*18,24,25*). Because the time point of initiation of inflammation is not always known, a target that is upregulated early and is stable for a long period should be advantageous. However, a basal level of ICAM-1 exists that could yield high background (*18*). In contrast, E-selectin appears to be upregulated only during inflammation (*2*). We did observe a high level of ^{111}In activity in the major organs (liver, spleen and kidney), which would make detection of inflammation in these organs difficult. This problem also occurs in both ^{111}In-labeled polyclonal IgG and ^{111}In-labeled WBCs (*26,27*). Most detection techniques utilizing antibodies are handicapped by high blood background, which can obscure lesions (*13,28,29*). The biggest advantage of ^{111}In-ICAM-1 is its rapid disappearance from the blood and low value of circulating activity at 4 hr. At 4 hr, the percent ID per gram of ^{111}In-aICAM-1 in the blood was 30%–40% of that for ^{111}In-labeled human polyclonal IgG obtained in rats (*15,16*), implying a superior background compared with this new radiopharmaceutical. The images also indicate that bone and muscle uptake are low at both 1 and 18 hr. Finally, the presence of soluble ICAM-1 and E-selectin in the blood, which is elevated in certain inflammatory processes, could interfere with localization by binding available antibody in the circulation (*6*). Our preliminary evidence suggests, however, that ^{111}In-aICAM-1 can function as an early (approximately 4 hr) indicator of disease in the bleomycin model of acute and chronic lung injury (*30*). Indium-111-aICAM-1 levels were elevated in injured lung before the detection of lung leakage and yielded a 8:1 target/background ratio. Labeled aICAM-1 has also been used successfully to detect heart and lung transplant rejection in animal models (*31–33*).

These anti-adhesion molecule probes may also shed light on the mechanism of WBC trafficking in vivo. Implicit in the work of Doerschuk et al. (*34*) is that ^{111}In-labeled WBCs can be used to monitor WBC kinetics. In contrast, Ussov et al. (*35*) and McAfee et al. (*36*) showed that ^{111}In labeling activates or damages WBCs, and care in labeling must be taken so that these cells accurately reflect the movement of unlabeled cells. Because ^{111}In-aICAM-1 appears to detect ICAM-1 in vivo, this and other probes may provide an alternative means to assess WBC kinetics. In that vein, Ussov et al. (*35*) suggested that increased adhesiveness may be a factor in the diffusely increased ^{111}In-labeled WBC lung uptake on early images. Our data, demonstrating initially high levels of ICAM-1 in the lung, would be consistent with this suggestion if the labeling process upregulates LFA-1 α on PMNs.

CONCLUSION

The biodistribution of ^{111}In-aICAM-1 demonstrates that this probe can detect constitutively expressed ICAM-1 in various organs. The role of ICAM-1 as a very early event in the inflammatory process suggests that this antibody may be useful as an early detector of acute infections. Whether this will be possible will require investigations using a number of different model systems. These studies are presently in progress.

ACKNOWLEDGMENTS

We thank U. Ryan, PhD, T Cell Science, Inc., Cambridge, MA, for his donation of the rat lung microvascular endothelial cells. This work was supported in part by Faculty Research Grants from the University of Connecticut Health Center. Immunofluorescence images were obtained at the Center for Biomedical Imaging Technology at the University of Connecticut Health Center. A preliminary account of this data has been presented elsewhere (*37*).

REFERENCES

1. Guyton AC. *Textbook of medical physiology*, 8th ed. Philadelphia: WB Saunders; 1991:365–372.
2. Zimmerman GA, Prescott SM, McIntyre TM. Endothelial cell interactions with granulocytes: tethering and signaling molecules. *Immunol Today* 1992;13:93–100.
3. Springer TA. Adhesion receptors of the immune system. *Nature* 1990;346:425–434.
4. Smith CW, Marlin SD, Rothlein R, et al. Cooperative interactions of LFA-1 and Mac-1 with intercellular adhesion molecule-1 in facilitating adherence and transendothelial migration of human neutrophils in vitro. *J Clin Invest* 1989;83:2008–2017.
5. Argenbright LW, Barton RW. Interactions of leukocyte integrins with intercellular adhesion molecule 1 in the production of inflammatory vascular injury in vivo. *J Clin Invest* 1992;89:259–272.
6. Gearing AJH, Newman W. Circulating adhesion molecules in disease. *Immunol Today* 1993;14:506–512.
7. Pohlman TH, Stanness KA, Beatty PG, et al. An endothelial cell surface factor induced in vitro by lipopolysaccharide, interleukin-1 and tumor necrosis factor increases neutrophil adherence by a CDw18-dependent mechanism. *J Immunol* 1986;136:4548–4553.
8. Wellicome SM, Thornbill MH, Pitzalis C, et al. A monoclonal antibody that detects a novel antigen on endothelial cells and is induced by TFNα, IL-1 or LPS. *J Immunol* 1990;144:2558–2565.
9. Keelan ETM, Harrison AA, Chapman PT, et al. Imaging vascular endothelial activation: an approach using radiolabeled monoclonal antibodies against the endothelial cell adhesion molecule E-selectin. *J Nucl Med* 1994;35:276–281.
10. Paik CH, Ebbert MA, Murphy PR, et al. Factors influencing DTPA conjugation with antibodies by cyclic DTPA anhydride. *J Nucl Med* 1983;24:1158–1163.
11. Baker HJ, Lindsey JR, Weisbroth, SH. *The laboratory rat*, vol. II: *research applications*. New York: Academic Press; 1980:257.
12. Syrbu S, Thrall RS, Wisniecki P, Lifchez S, Smilowitz HM. Increased immunoreactive rat lung ICAM-1 in oleic acid induced lung injury. *Exp Lung Res* 1995;21:599–616.
13. Goodwin DA. Pharmacokinetics and antibodies. *J Nucl Med* 1987;8:1358–1362.
14. Eisen HN. Antigen-Antibody reactions. In: Davis BD, Dulbecco R, Eisen HN, Gindberg HS, eds. *Microbiology*, 3rd ed. Hagerstown, MD: Harper & Row; 1980: 298–336.
15. Oyen WJG, Claessens RAMJ, van der Meer JWM, et al. Biodistribution and kinetics of radiolabeled proteins in rates with focal infection. *J Nucl Med* 1992;33:388–394.
16. Abrams MJ, Juweid M, tenKate CI, et al. Technetium-99m-human polyclonal IgG radiolabeled via the hydrazino nicotinamide derivative for imaging focal sites of infection in rats. *J Nucl Med* 1990;31:2022–2028.
17. Luscinskas FW, Cybulsky MI, Keily J-M, et al. Cytokine-activated human endothelial monolayers support enhanced neutrophil transmigration via a mechanism involving both endothelial-leukocyte adhesion molecule-1 and intercellular adhesion molecule-1. *J Immunol* 1991;146:1617–1625.
18. Dustin ML, Rothlein R, Bhan AK, et al. Induction by IL-1 and interferon-γ: tissue distribution biochemistry, and function of a natural adherence molecule (ICAM-1). *J Immunol* 1986;137:245–254.

19. Montefort S, Roche WR, Howarth PH, et al. Intercellular adhesion molecule-1 (ICAM-1) and endothelial leucocyte adhesion molecule-1 (ELAM-1) expression in the bronchial mucosa of normal and asthmatic subjects. *Eur Respir J* 1992;5:815–823.
20. Keelan ETM, Licence ST, Peters AM, et al. Characterization of E-selectin expression in vivo with use of a radiolabeled monoclonal antibody. *Am J Physiol* 1994;266:H279–H290.
21. Mountford PJ, Kettle AG, O'Doherty MJ, Coakley AJ. Comparison of technetium-99m-HMPAO leukocytes with indium-111-oxine leukocytes for localizing intraabdominal sepsis. *J Nucl Med* 1990;31:311–315.
22. Roddie ME, Peters AM, Danpure HJ, et al. Inflammation: imaging with Tc-99m HMPAO-labeled leukocytes. *Radiology* 1988;166:767–772.
23. Reynolds JH, Graham D, Smith FW. Imaging inflammation with ^{99m}Tc-HMPAO-labeled leucocytes. *Clin Radiol* 1990;42:195–198.
24. Leeuwenberg JFM, Smeets EF, Neefjes JJ, et al. E-selectin and intercellular adhesion molecule-1 are released by activated human endothelial cells in vitro. *Immunology* 1992;77:543–549.
25. Norris P, Poston RN, Thomas S, Thornhill M, Hawk J, Haskard DO. The expression of endothelial leukocyte adhesion molecule-1 (ELAM-1), intercellular adhesion molecule-1 (ICAM-1) and vascular cell adhesion molecule-1 (VCAM-1) in experimental cutaneous inflammation: a comparison of ultraviolet B erythema and delayed hypersensitivity. *J Invest Dermatol* 1991;96:763–770.
26. Serafini AN, Garty I, Vargas-Cuba R, et al. Clinical evaluation of a scintigraphic method for diagnosing inflammations/infections using indium-111-labeled nonspecific human IgG. *J Nucl Med* 1991;32:2227–2232.
27. Becker W, Schomann E, Fischback W, et al. Comparison of ^{99}Tc-HMPAO and ^{111}In-oxine-labeled granulocytes in man: first clinical results. *Nucl Med Commun* 1988;9:435–447.
28. Hnatowich DJ. Antibody radiolabeling, problems and promises. *Nucl Med Biol* 1990;17:49–55.
29. Oyen WJG, Claessens RAMJ, van Horn JR, et al. Scintigraphic detection of bone and joint infections with indium-111-labeled nonspecific polyclonal human immunoglobulin G. *J Nucl Med* 1990;31:430–412.
30. Sasso D, Gionfriddo M, Syrbu S, Smilowitz H, Thrall R, Weiner R. Early detection of ARDS using In-111 labeled anti-intercellular adhesion molecule-1 in a rat model [Abstract]. *J Nucl Med* 1995;36(suppl):159P.
31. Hiroe M, Ohta Y, Miyasaka M, et al. Myocardial uptake of radiolabeled monoclonal anti-intercellular adhesion molecule-1, antibody in detecting acute myocardial infarction of rat [Abstract]. *J Nucl Med* 1993;34(suppl):66P.
32. Hiroe M, Ohta Y, Amano J, et al. Uptake of indium-111 labeled anti-intercellular adhesion molecule-1 antibody in early detection of lung allograft rejection in rats [Abstract]. *J Nucl Med* 1994;34(suppl):239P.
33. Ohtani H, Strauss HW, Southern JF, et al. Imaging of intercellular adhesion molecule-1 induction in rejecting heart: a new scintigraphic approach to detect early allograft rejection. *Transplant Proc* 1993;25:867–869.
34. Doerschuk CM, Beyers N, Coxson HO, et al. Comparison of neutrophil and capillary diameters and their relation to neutrophil sequestration in the lung. *J Appl Physiol* 1993;74:3040–4045.
35. Ussov WY, Peters AM, Hodgson HJF, Hughes JMB. Quantification of pulmonary uptake of indium-111 labeled granulocyte in inflammatory bowel disease. *Eur J Nucl Med* 1994;21:6–11.
36. McAfee JG, Gagne GM, Subramanian G, et al. Distribution of leukocytes labeled with In-111 oxine in dogs with acute inflammatory lesions. *J Nucl Med* 1980;21:1059–1068.
37. Sasso D, Gionfriddo M, Thrall RS, Syrbu S, Smilowitz HM, Weiner RE. Biodistribution of antibody directed against intracellular adhesion molecule-1 in normal rats [Abstract]. *Am J Respir Crit Care Med* 1995;171(suppl):A70.

HMPAO as a Regional Cerebral Blood Flow Tracer at High Flow Levels

Roderick Duncan, James Patterson and I. Mhairi Macrae

Departments of Neurology and Clinical Physics, Institute of Neurological Sciences, Southern General Hospital NHS Trust, Glasgow; and Wellcome Surgical Institute, University of Glasgow, Glasgow, Scotland

HMPAO is being used extensively to image rCBF during focal seizures in humans. It is, however, theoretically possible that backdiffusion of tracer causes retention to fall as flow rises at high levels. **Methods:** We used a double label ^{99m}Tc-HMPAO/^{14}C-IAP autoradiographic technique to compare HMPAO retention and regional cerebral blood flow in penicillin induced focal seizures in rats. **Results:** Using this protocol, flows of up to 717 ml/100 g per min were observed. The same pattern of uptake was seen on IAP and HMPAO autoradiographs, with the exception of relatively high HMPAO uptake in the choroid plexus, in the fissures and, in one animal only, the supramammilary nucleus. Correlation of HMPAO retention and blood flow showed a linear relationship up to 200 ml/100 g per min in all animals. HMPAO retention then showed a falloff in its rise with blood flow, but was still increasing, even at the highest flows seen. At 700 ml/100 g/min, HMPAO retention was 20% of that expected from a linear relationship. **Conclusion:** HMPAO is a suitable tracer of rCBF at high flows and is unlikely to produce anomalous images in human focal seizures.

Key Words: epilepsy; penicillin; rCBF; technetium-99m-HMPAO

J Nucl Med 1996; 37:661–664

HMPAO (*1*) is a lipophilic compound that can be labeled with ^{99m}Tc and used as a tracer of regional cerebral blood flow (rCBF). After intravenous injection, it crosses the blood-brain barrier freely. Thereafter, it becomes less lipophilic and less able to re-cross cellular membranes and the blood-brain barrier. Therefore, the distribution of HMPAO in the brain reflects rCBF and remains stable for some hours.

The brain distribution of microspheres and ^{99m}Tc-HMPAO correlate well in the dog (*2*), and previous autoradiographic studies using iodoantipyrine (IAP) have also shown good agreement (*3,4*). Initial uptake in the normal human brain appears to be proportional to rCBF (*5*), and to correspond well with rCBF as shown by other in vivo methods, such as ^{133}Xe (*6,7*) and PET (*8,9*).

The conversion of HMPAO to a less lipophilic compound takes place with an exponential half life of 40 sec. Thus, at high flow rates, there is a backdiffusion effect, causing HMPAO uptake to underestimate flow. Lassen et al. (*5*) proposed a correction which can partially compensate for this effect.

Ictal HMPAO-SPECT is now being used extensively to localize epileptic foci prior to surgical resection (*10,11*). Although human data is scant, animal work has shown ictal rises in rCBF in generalized seizures of up to 900% (*12*). At these extremely high flow rates (up to 1000 ml/100 g per min in absolute terms), it is important to verify that HMPAO retention in neurones does not begin to fall as flow rises, as the same ^{99m}Tc activity might then be seen at two different flow rates. A recent publication (*13*) has underlined the need to verify the accuracy of the technique in specific pathological situations.

This study aims to compare HMPAO uptake with rCBF as measured by IAP uptake over the large range of flows achieved using the penicillin model of focal epilepsy in the rat.

Received Feb. 10, 1995; revision accepted Jul. 14, 1995.

For correspondence or reprints contact: Roderick Duncan, MD, Department of Neurology, Institute of Neurological Sciences, Southern General Hospital, Glasgow, Scotland G51 4TF.